

Search for R-parity violating decays of supersymmetric particles in e^+e^- collisions at centre-of-mass energies from 189 GeV to 202 GeV

The ALEPH Collaboration

R. Barate, D. Decamp, P. Ghez, C. Goy, S. Jezequel, J.-P. Lees, F. Martin, E. Merle, M.-N. Minard, B. Pietrzyk

Laboratoire de Physique des Particules (LAPP), IN²P³-CNRS, 74019 Annecy-le-Vieux Cedex, France

S. Bravo, M.P. Casado, M. Chmeissani, J.M. Crespo, E. Fernandez, M. Fernandez-Bosman, Ll. Garrido¹⁵, E. Graugés, J. Lopez, M. Martinez, G. Merino, R. Miquel, Ll.M. Mir, A. Pacheco, D. Paneque, H. Ruiz
Institut de Física d'Altes Energies, Universitat Autònoma de Barcelona, 08193 Bellaterra (Barcelona), Spain⁷

A. Colaleo, D. Creanza, N. De Filippis, M. de Palma, G. Iaselli, G. Maggi, M. Maggi¹, S. Nuzzo, A. Ranieri, G. Raso²⁴, F. Ruggieri, G. Selvaggi, L. Silvestris, P. Tempesta, A. Tricomi³, G. Zito
Dipartimento di Fisica, INFN Sezione di Bari, 70126 Bari, Italy

X. Huang, J. Lin, Q. Ouyang, T. Wang, Y. Xie, R. Xu, S. Xue, J. Zhang, L. Zhang, W. Zhao
Institute of High Energy Physics, Academia Sinica, Beijing, P.R. China⁸

D. Abbaneo, P. Azzurri, G. Boix⁶, O. Buchmüller, M. Cattaneo, F. Cerutti, B. Clerbaux, G. Dissertori, H. Drevermann, R.W. Forty, M. Frank, F. Gianotti, T.C. Greening, J.B. Hansen, J. Harvey, D.E. Hutchcroft, P. Janot, B. Jost, M. Kado, V. Lemaître, P. Maley, P. Mato, A. Minten, A. Moutoussi, F. Ranjard, L. Rolandi, D. Schlatter, M. Schmitt²⁰, O. Schneider², P. Spagnolo, W. Tejessy, F. Teubert, E. Tournefier²⁶, A. Valassi, J.J. Ward, A.E. Wright

European Laboratory for Particle Physics (CERN), 1211 Geneva 23, Switzerland

Z. Ajaltouni, F. Badaud, S. Dessagne, A. Falvard, D. Fayolle, P. Gay, P. Henrard, J. Jousset, B. Michel, S. Monteil, J.-C. Montret, D. Pallin, J.M. Pascolo, P. Perret, F. Podlyski

Laboratoire de Physique Corpusculaire, Université Blaise Pascal, IN²P³-CNRS, Clermont-Ferrand, 63177 Aubière, France

J.D. Hansen, J.R. Hansen, P.H. Hansen, B.S. Nilsson, A. Wäänänen
Niels Bohr Institute, 2100 Copenhagen, Denmark⁹

G. Daskalakis, A. Kyriakis, C. Markou, E. Simopoulou, A. Vayaki
Nuclear Research Center Demokritos (NRCD), 15310 Attiki, Greece

A. Blondel¹², J.-C. Brient, F. Machefert, A. Rougé, M. Swynghedauw, R. Tanaka, H. Videau
Laboratoire de Physique Nucléaire et des Hautes Energies, Ecole Polytechnique, IN²P³-CNRS, 91128 Palaiseau Cedex, France

E. Focardi, G. Parrini, K. Zachariadou

Dipartimento di Fisica, Università di Firenze, INFN Sezione di Firenze, 50125 Firenze, Italy

A. Antonelli, M. Antonelli, G. Bencivenni, G. Bologna⁴, F. Bossi, P. Campana, G. Capon, V. Chiarella, P. Laurelli, G. Mannocchi⁵, F. Murtas, G.P. Murtas, L. Passalacqua, M. Pepe-Altarelli²⁵
Laboratori Nazionali dell'INFN (LNF-INFN), 00044 Frascati, Italy

M. Chalmers, A.W. Halley, J. Kennedy, J.G. Lynch, P. Negus, V. O'Shea, B. Raeven, D. Smith, P. Teixeira-Dias, A.S. Thompson

Department of Physics and Astronomy, University of Glasgow, Glasgow G12 8QQ, UK¹⁰

R. Cavanaugh, S. Dhamotharan, C. Geweniger, P. Hanke, V. Hepp, E.E. Kluge, G. Leibenguth, A. Putzer, K. Tittel, S. Werner¹⁹, M. Wunsch¹⁹

Kirchhoff-Institut für Physik, Universität Heidelberg, 69120 Heidelberg, Germany¹⁶

R. Beuselinck, D.M. Binnie, W. Cameron, G. Davies, P.J. Dornan, M. Girone¹, N. Marinelli, J. Nowell, H. Przysiezniak, J.K. Sedgbeer, J.C. Thompson¹⁴, E. Thomson²³, R. White

Department of Physics, Imperial College, London SW7 2BZ, UK¹⁰

V.M. Ghete, P. Girtler, E. Kneringer, D. Kuhn, G. Rudolph

Institut für Experimentalphysik, Universität Innsbruck, 6020 Innsbruck, Austria¹⁸

E. Bouhova-Thacker, C.K. Bowdery, D.P. Clarke, G. Ellis, A.J. Finch, F. Foster, G. Hughes, R.W.L. Jones¹, M.R. Pearson, N.A. Robertson, M. Smizanska

Department of Physics, University of Lancaster, Lancaster LA1 4YB, UK¹⁰

I. Giehl, F. Hölldorfer, K. Jakobs, K. Kleinknecht, M. Kröcker, A.-S. Müller, H.-A. Nürnbergger, G. Quast¹, B. Renk, E. Rohne, H.-G. Sander, S. Schmeling, H. Wachsmuth, C. Zeitnitz, T. Ziegler

Institut für Physik, Universität Mainz, 55099 Mainz, Germany¹⁶

A. Bonissent, J. Carr, P. Coyle, C. Curtil, A. Ealet, D. Fouchez, O. Leroy, T. Kachelhoffer, P. Payre, D. Rousseau, A. Tilquin

Centre de Physique des Particules de Marseille, Univ Méditerranée, IN²P³-CNRS, 13288 Marseille, France

M. Aleppo, S. Gilardoni, F. Ragusa

Dipartimento di Fisica, Università di Milano e INFN Sezione di Milano, 20133 Milano, Italy

A. David, H. Dietl, G. Ganis²⁷, A. Heister, K. Hüttmann, G. Lütjens, C. Mannert, W. Männer, H.-G. Moser, S. Schael, R. Settles¹, H. Stenzel, W. Wiedenmann, G. Wolf

Max-Planck-Institut für Physik, Werner-Heisenberg-Institut, 80805 München, Germany¹⁶

J. Boucrot¹, O. Callot, M. Davier, L. Duflot, J.-F. Grivaz, Ph. Heusse, A. Jacholkowska¹, L. Serin, J.-J. Veillet, I. Videau, J.-B. de Vivie de Régie²⁸, C. Yuan, D. Zerwas

Laboratoire de l'Accélérateur Linéaire, Université de Paris-Sud, IN²P³-CNRS, 91898 Orsay Cedex, France

G. Bagliesi, T. Boccali, G. Calderini, V. Ciulli, L. Foà, A. Giammanco, A. Giassi, F. Ligabue, A. Messineo, F. Palla¹, G. Sanguinetti, A. Sciabà, G. Sguazzoni, R. Tenchini¹, A. Venturi, P.G. Verdini

Dipartimento di Fisica dell'Università, INFN Sezione di Pisa, e Scuola Normale Superiore, 56010 Pisa, Italy

G.A. Blair, J. Coles, G. Cowan, M.G. Green, L.T. Jones, T. Medcalf, J.A. Strong, J.H. von Wimmersperg-Toeller

Department of Physics, Royal Holloway & Bedford New College, University of London, Surrey TW20 OEX, UK¹⁰

R.W. Clift, T.R. Edgecock, P.R. Norton, I.R. Tomalin

Particle Physics Dept., Rutherford Appleton Laboratory, Chilton, Didcot, Oxon OX11 0QX, UK¹⁰

B. Bloch-Devaux¹, D. Boumediene, P. Colas, B. Fabbro, E. Lançon, M.-C. Lemaire, E. Locci, P. Perez, J. Rander, J.-F. Renardy, A. Rosowsky, P. Seager¹³, A. Trabelsi²¹, B. Tuchming, B. Vallage

CEA, DAPNIA/Service de Physique des Particules, CE-Saclay, 91191 Gif-sur-Yvette Cedex, France¹⁷

N. Konstantinidis, C. Loomis, A.M. Litke, G. Taylor

Institute for Particle Physics, University of California at Santa Cruz, Santa Cruz, CA 95064, USA²²

C.N. Booth, S. Cartwright, F. Combley, P.N. Hodgson, M. Lehto, L.F. Thompson

Department of Physics, University of Sheffield, Sheffield S3 7RH, UK¹⁰

K. Affholderbach, A. Böhrer, S. Brandt, C. Grupen, J. Hess, A. Misiejuk, G. Prange, U. Sieler

Fachbereich Physik, Universität Siegen, 57068 Siegen, Germany¹⁶

C. Borean, G. Giannini, B. Gobbo

Dipartimento di Fisica, Università di Trieste e INFN Sezione di Trieste, 34127 Trieste, Italy

H. He, J. Putz, J. Rothberg, S. Wasserbaech

Experimental Elementary Particle Physics, University of Washington, Seattle, WA 98195, USA

S.R. Armstrong, K. Cranmer, P. Elmer, D.P.S. Ferguson, Y. Gao, S. González, O.J. Hayes, H. Hu, S. Jin, J. Kile, P.A. McNamara III, J. Nielsen, W. Orejudos, Y.B. Pan, Y. Saadi, I.J. Scott, J. Walsh, J. Wu, Sau Lan Wu, X. Wu, G. Zobernig

Department of Physics, University of Wisconsin, Madison, WI 53706, USA¹¹

Received: 26 October 2000 / Published online: 23 March 2001 – © Springer-Verlag 2001

Abstract. Searches for the production of supersymmetric particles under the assumption that R-parity is violated via a single dominant $LL\bar{E}$, $LQ\bar{D}$ or $\bar{U}\bar{D}\bar{D}$ coupling were performed. These use the data collected by the ALEPH detector at LEP at centre-of-mass energies from 188.6 to 201.6 GeV. The numbers

of candidate events observed in the data are consistent with Standard Model expectations. Upper limits on the production cross sections and lower limits on the masses of charginos, sleptons, squarks and sneutrinos are derived.

1 Introduction

Minimal supersymmetric extensions of the Standard Model (MSSM) [1] usually make the assumption that R-parity, $R_p = -1^{3B+L+2S}$, is conserved [2], where B denotes the baryon number, L the lepton number and S the spin of a field. The conservation of R-parity is not required theoretically and models in which R-parity is violated can be constructed which are compatible with existing experimental constraints.

¹ Also at CERN, 1211 Geneva 23, Switzerland

² Now at Université de Lausanne, 1015 Lausanne, Switzerland

³ Also at Dipartimento di Fisica di Catania and INFN Sezione di Catania, 95129 Catania, Italy

⁴ Deceased

⁵ Also Istituto di Cosmo-Geofisica del C.N.R., Torino, Italy

⁶ Supported by the Commission of the European Communities, contract ERBFMBICT982894

⁷ Supported by CICYT, Spain

⁸ Supported by the National Science Foundation of China

⁹ Supported by the Danish Natural Science Research Council

¹⁰ Supported by the UK Particle Physics and Astronomy Research Council

¹¹ Supported by the US Department of Energy, grant DE-FG0295-ER40896

¹² Now at Departement de Physique Corpusculaire, Université de Genève, 1211 Genève 4, Switzerland

¹³ Supported by the Commission of the European Communities, contract ERBFMBICT982874

¹⁴ Also at Rutherford Appleton Laboratory, Chilton, Didcot, UK

¹⁵ Permanent address: Universitat de Barcelona, 08208 Barcelona, Spain

¹⁶ Supported by the Bundesministerium für Bildung, Wissenschaft, Forschung und Technologie, Germany

¹⁷ Supported by the Direction des Sciences de la Matière, C.E.A

¹⁸ Supported by the Austrian Ministry for Science and Transport

¹⁹ Now at SAP AG, 69185 Walldorf, Germany

²⁰ Now at Harvard University, Cambridge, MA 02138, USA

²¹ Now at Département de Physique, Faculté des Sciences de Tunis, 1060 Le Belvédère, Tunisia

²² Supported by the US Department of Energy, grant DE-FG03-92ER40689

²³ Now at Department of Physics, Ohio State University, Columbus, OH 43210-1106, USA

²⁴ Also at Dipartimento di Fisica e Tecnologia Relative, Università di Palermo, Palermo, Italy

²⁵ Now at CERN, 1211 Geneva 23, Switzerland

²⁶ Now at ISN, Institut des Sciences Nucléaires, 53 Av. des Martyrs, 38026 Grenoble, France

²⁷ Now at Università degli Studi di Roma Tor Vergata, Dipartimento di Fisica, 00133 Roma, Italy

²⁸ Now at Centre de Physique des Particules de Marseille, Univ Méditerranée, F-13288 Marseille, France

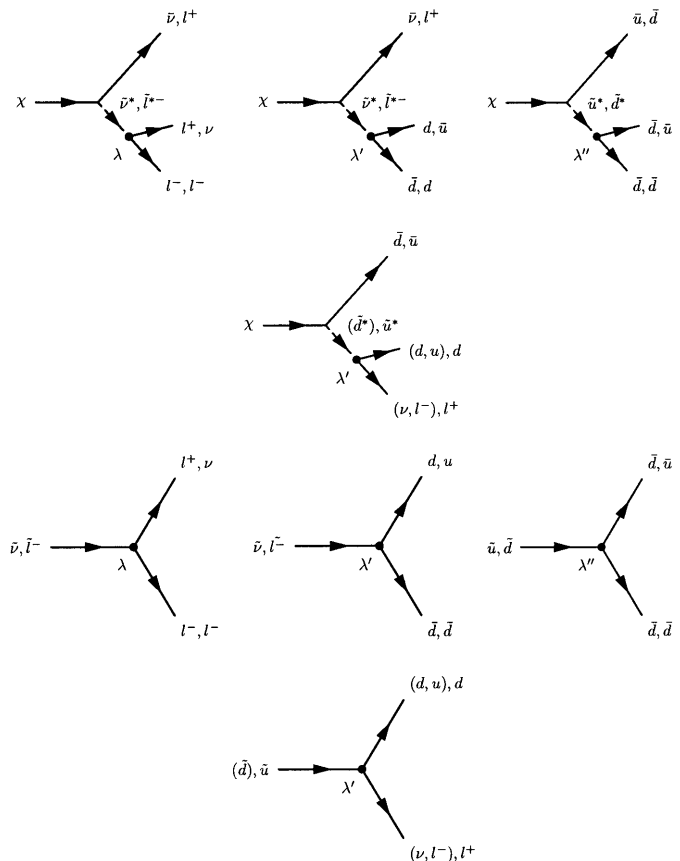


Fig. 1. Direct R-parity violating decays of supersymmetric particles via the λ , λ' and λ'' couplings. The points mark the R-parity violating vertex in the decay

The R-parity violating terms of the superpotential considered here are [3]

$$W_{\mathcal{R}_p} = \lambda_{ijk} L_i L_j \bar{E}_k + \lambda'_{ijk} L_i Q_j \bar{D}_k + \lambda''_{ijk} \bar{U}_i \bar{D}_j \bar{D}_k, \quad (1)$$

where \bar{D} , \bar{U} (\bar{E}) are the down-like and up-like quark (lepton) singlet superfields, and Q (L) is the quark (lepton) doublet superfield respectively; λ , λ' and λ'' are Yukawa couplings and $i, j, k = 1, 2, 3$ are generation indices. The presence of such R-parity violating terms imply that the lightest supersymmetric particle (LSP) is no longer stable and that sparticles can be produced singly. The sparticle decays which proceed directly to standard model particles are called *direct* decays. Decays in which the sparticle first decays, conserving R-parity, to the lightest neutralino are referred to as *indirect* decays. Both cases are illustrated in Fig. 1. Other cascade decays are possible but not considered in the following.

In this paper a new search for the resonant production of single sneutrinos decaying indirectly is presented. In addition, previously reported searches for both direct and

Table 1. For each sparticle the table lists whether the decay mode is searched for (\bullet), possible but not considered (\diamond), or not possible (\times). Those processes marked with \dagger were not considered in the 183 GeV results [4]

	$LL\bar{E}$		$LQ\bar{D}$		$\bar{U}\bar{D}\bar{D}$	
	Direct	Indirect	Direct	Indirect	Direct	Indirect
χ^\pm	\diamond	\bullet	\diamond	\bullet	\diamond	\bullet
χ'	\diamond	\bullet	\diamond	\bullet	\diamond	\bullet
$\tilde{e}, \tilde{\mu}, \tilde{\tau}$	\bullet	\bullet	$\bullet(\tilde{L})$	\dagger	\times	\bullet
$\tilde{\nu}_e, \tilde{\nu}_\mu, \tilde{\nu}_\tau$	\bullet	\bullet	\bullet	\dagger	\times	\bullet
\tilde{u}	\times	\bullet	\bullet	\dagger	$\bullet(\tilde{u}_R)$	\bullet
\tilde{d}	\times	\bullet	\bullet	\dagger	$\bullet(\tilde{d}_R)$	\bullet

indirect decays of pair produced sparticles at 183 GeV [4] are extended and applied to new data at higher energies. In particular, new selections for indirect decays of sleptons and squarks via the $LQ\bar{D}$ operator are developed. Table 1 summarises the possible decays and indicates those addressed in this paper. Other collaborations at LEP have published similar searches at lower energies [5–9].

The following assumptions are made throughout:

- All three terms in (1) are addressed, however only one term for a specific set of indices (i, j and k) is considered non zero. Unless otherwise stated the derived limits correspond to the choice of indices for the coupling giving the worst limit.
- The lifetime of the sparticles can be neglected, i.e. the mean flight path is less than 1 cm.
- Results are interpreted within the framework of the MSSM. Gaugino mass unification at the electroweak scale is assumed, giving the condition $M_1 = \frac{5}{3}M_2 \tan^2 \theta_W$.
- For the case of the charginos and neutralinos, only large values of the universal scalar mass m_0 are considered; this implies the *direct* decays of the lightest chargino and the next-to-lightest neutralino are suppressed. It also implies three-body decay kinematics for the lightest neutralino.

The search results reported here use data collected by the ALEPH detector in 1998 and 1999 from e^+e^- collisions at centre-of-mass energies between 188.6 GeV and 201.6 GeV. The total data sample used corresponds to an integrated recorded luminosity of 173.6 pb^{-1} at 188.6 GeV, 29.0 pb^{-1} at 191.6 GeV, 80.1 pb^{-1} at 195.5 GeV, 85.9 pb^{-1} at 199.5 GeV and 41.9 pb^{-1} at 201.6 GeV.

This paper is organised as follows: after a brief description of the ALEPH detector in Sect. 2, the Monte Carlo samples used for signal and background generation are detailed in Sect. 3. Sections 4, 5 and 6 give the results and interpretations for each of the R-parity violating couplings, and finally Sect. 7 gives a summary of the results.

2 The ALEPH detector

The ALEPH detector is described in detail in [10]. An account of the performance of the detector and a description of the standard analysis algorithms can be found in [11]. Here, only a brief description of the detector components and the algorithms relevant for this analysis is given.

The trajectories of charged particles are measured with a silicon vertex detector, a cylindrical drift chamber, and a large time projection chamber (TPC). The central detectors are immersed in a 1.5 T axial magnetic field provided by a superconducting solenoidal coil. The electromagnetic calorimeter (ECAL), placed between the TPC and the coil, is a highly segmented sampling calorimeter which is used to identify electrons and photons and to measure their energies. The luminosity monitors extend the calorimetric coverage down to 34 mrad from the beam axis. The hadron calorimeter (HCAL) consists of the iron return yoke of the magnet instrumented with streamer tubes. It provides a measurement of hadronic energy and, together with the external muon chambers, muon identification. The calorimetric and tracking information are combined in an energy flow algorithm which gives a measure of the total energy, and therefore the missing energy, with an uncertainty of $(0.6\sqrt{E} + 0.6)$ GeV.

Electron identification is primarily based upon the matching between the measured momentum of the charged track and the energy deposited in the ECAL. Additional information from the shower profile in the ECAL and the measured rate of specific ionisation energy loss in the TPC are also used. Muons are separated from hadrons by their characteristic pattern in HCAL and the presence of associated hits in the muon chambers.

3 Monte Carlo samples and efficiencies

The signal topologies were simulated using the SUSYGEN Monte Carlo program [12] modified as described in [4]. The events were subsequently passed through either a full simulation or a faster simplified simulation of the ALEPH detector. Where the fast simulation was used a subselection of these were also passed through the full simulation to verify the accuracy of the fast simulation.

Samples of all major backgrounds were generated and passed through the full simulation, corresponding to at least 10 times the collected luminosity in the data. The PYTHIA generator [13] was used to produce $q\bar{q}$ events and four-fermion final states from $W\nu$, ZZ and Zee , with a vector-boson invariant mass cut of $0.2 \text{ GeV}/c^2$ for ZZ and $W\nu$, and $2 \text{ GeV}/c^2$ for Zee . Pairs of W bosons were generated with KORALW [14]. The KORALW cross sections were adjusted to agree with the most recent theoretical calculations [15]. Pair production of leptons was simulated with UNIBAB [16] (electrons) and KORALZ [17] (muons and taus). The $\gamma\gamma \rightarrow f\bar{f}$ processes were generated with PHOTO2 [18].

The selections were optimised to give the minimum expected 95% C.L. excluded cross section in the absence of a signal for masses close to the high end of the expected sensitivity. Selection efficiencies were determined

as a function of the SUSY particle masses and the generation structure of the R-parity violating couplings λ_{ijk} , λ'_{ijk} and λ''_{ijk} .

The cross section limits were evaluated at the highest centre-of-mass energy. Where data taken at a range of centre-of-mass energies contributed to the exclusions the data were weighted with the expected evolution of the cross-section with \sqrt{s} .

The systematic uncertainties on the selection efficiencies are of order of 4–5% and are dominated by the statistical uncertainty of the Monte Carlo signal samples, with small additional contributions from lepton identification and energy flow reconstruction. They were taken into account by reducing the selection efficiencies by one standard deviation of the statistical error.

When setting the limits, background subtraction was performed for two- and four-fermion final states according to the prescription given in [19]. Detailed comparisons of data and Monte Carlo predictions show systematic uncertainties in the Monte Carlo predictions. To take this uncertainty into account the amount of background subtracted is reduced. For two-fermion processes it was reduced by its statistical error. The contribution from WW and ZZ processes were reduced by the statistical error added in quadrature with 1% of its estimate. The components from $W\ell\nu$ and Zee processes were reduced by the statistical error added in quadrature 20% of their estimate. No background is subtracted for the $\gamma\gamma \rightarrow f\bar{f}$ processes.

4 Decays via a dominant $LL\bar{E}$ coupling

Under the assumption of a dominant $LL\bar{E}$ coupling, the decay topologies can consist of as little as two acoplanar leptons in the simplest case (direct slepton decay or single resonant sneutrino production), or they may consist of as many as six leptons plus four neutrinos in the most complicated case (indirect chargino decay). In addition to the purely leptonic topologies, the MSSM cascade decays of charginos into lighter neutralinos may produce multi-jet and multi-lepton final states. No direct decays are possible for the squarks.

The absolute lower limit on the mass of the lightest neutralino of 23 GeV/c^2 obtained in [20], which is valid for any choice of μ , M_2 , m_0 and generational indices (i , j and k), is used to restrict the range of neutralino mass considered for the indirect decays.

The various selections addressing the above topologies, the expected backgrounds, and the numbers of candidates selected in the data at $\sqrt{s} = 188.6\text{--}201.6$ GeV are summarised in Table 2. Details of the “6 Leptons + \cancel{E} ”, the “4 Leptons + \cancel{E} ” and the “4 Leptons” analyses are given in [20]. The “Acoplanar Leptons” and “Leptons and Hadrons” selections are described in [4], although the “Leptons and Hadrons” has been updated for the increased centre-of-mass energy as described in Sect. 4.2. Wherever the “Acoplanar Leptons” selection is used the expected combination of final state flavours (e, μ and τ) for each process is used to set the exclusion.

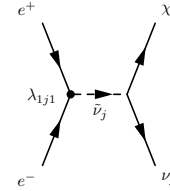


Fig. 2. Single sneutrino production via the λ_{1j1} coupling and subsequent *indirect* decay. The neutralino will subsequently decay via the first diagram in Fig. 1

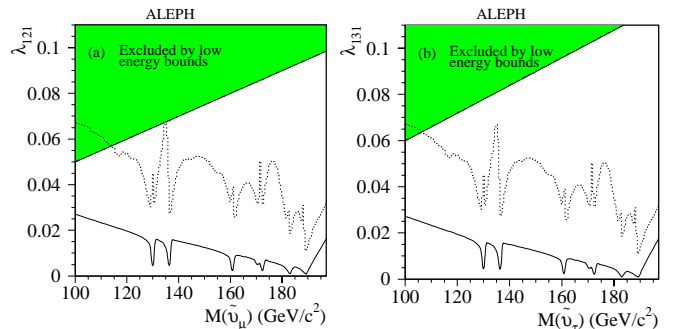


Fig. 3a,b. Plots **a** and **b** show the 95% C.L. upper limits on the value of the R-parity violating couplings, λ_{121} and λ_{131} , as a function of sneutrino mass for single sneutrino production and indirect decays (solid curve); the limits are shown for the neutralino mass giving the worst limit. For comparison the limit, assuming 100% branching ratio, for the direct decays to e^+e^- is also shown (dotted histogram). Assuming that $M(\tilde{\nu}_j) = M(\tilde{e}_R)$, the shaded region is excluded by **a** charged current universality and **b** R_τ . The exclusions are evaluated at $\mu = -200$ GeV/c^2 and $\tan\beta = 2$

4.1 Single resonant sneutrino production

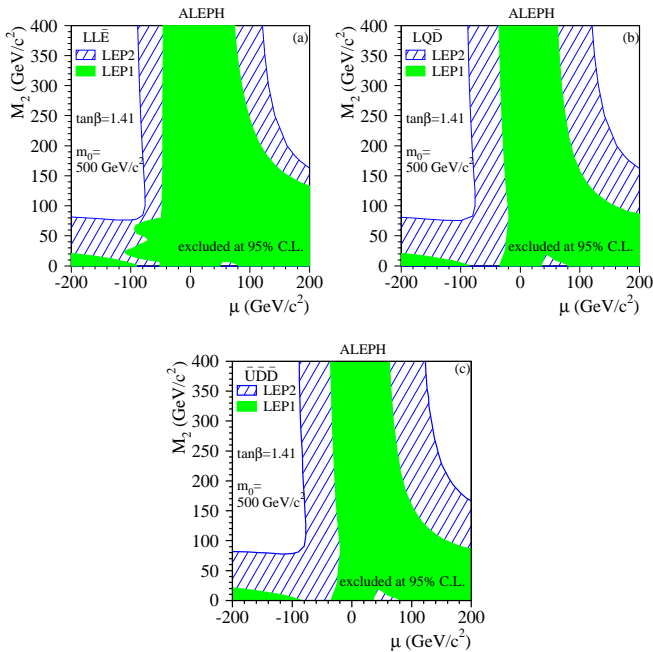
Single resonant production of sneutrinos [21] can occur for the specific couplings λ_{121} and λ_{131} . The sneutrino may decay indirectly through the diagram shown in Fig. 2 or directly to e^+e^- . A search for the direct decays using precision electroweak fits [22] has been performed. The search for indirect single sneutrino decays is presented here.

Since the production cross-section is a function of $|\lambda_{1j1}|^2$, limits can be set on the magnitude of λ_{1j1} as a function of the sneutrino mass. The best sensitivity is obtained for the case where the sneutrino is produced exactly on shell, $\sqrt{s} = M_{\tilde{\nu}}$. For centre-of-mass energies above $M_{\tilde{\nu}}$ initial state radiation from the e^+e^- system allows a radiative return to the sneutrino resonance. There is also some sensitivity for $M_{\tilde{\nu}} > \sqrt{s}$ via the production of a virtual sneutrino.

Since the final state consists of two leptons and two neutrinos the “Acoplanar Leptons” selection is used to select these events. The results of this selection are summarised in Table 2. Figure 3 shows the excluded values of λ_{121} and λ_{131} as a function of the mass of the sneutrinos; all data taken in the range $\sqrt{s} = 130$ to 189 GeV are used. The data and background numbers for the lower energies are given in [4, 20]. Also shown are the results for

Table 2. The observed numbers of events in the data and the corresponding Standard Model background expectations for the $LL\bar{E}$ selections

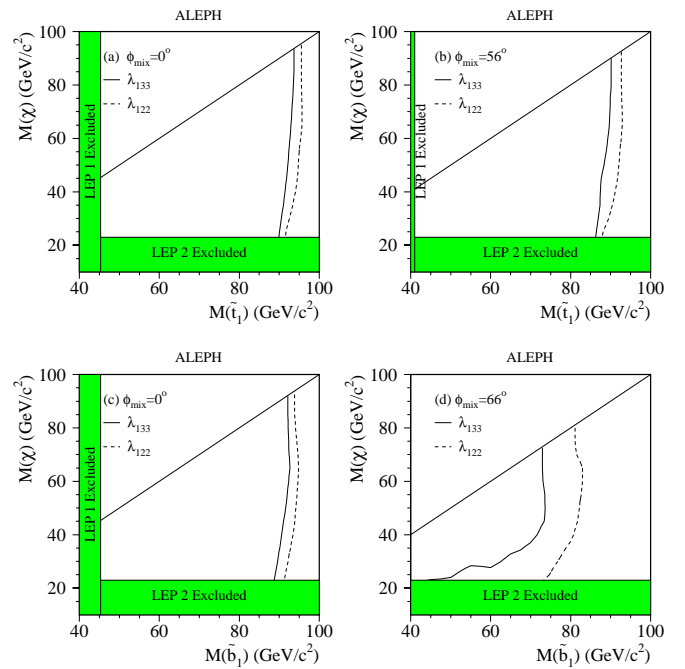
\sqrt{s} (GeV)	188.6		191.6		195.5		199.5		201.6		All	
Selection	Data	SM	Data	SM	Data	SM	Data	SM	Data	SM	Data	SM
Leptons and Hadrons	10	7.8	1	1.4	4	4.0	5	4.5	0	2.1	20	20
6 Leptons + \cancel{E}	2	1.0	1	0.2	0	0.4	0	0.5	0	0.2	3	2.2
4 Leptons + \cancel{E}	4	4.6	1	0.8	1	2.0	4	2.8	1	1.7	11	12
$llll$	3	5.1	1	0.7	3	1.7	8	2.3	0	1.3	15	11
$ll\tau\tau$	2	2.0	0	0.3	2	0.9	0	0.9	0	0.4	4	4.6
$\tau\tau\tau\tau$	5	4.2	1	0.7	1	1.9	5	2.1	0	1.1	12	10
Acoplanar Leptons	192	211	22	34	93	87	100	94	41	45	448	471

**Fig. 4a–c.** Regions in the (μ, M_2) plane excluded at 95% C.L. at $\tan\beta = 1.41$ and $m_0 = 500 \text{ GeV}/c^2$ for the three operators

the search for direct decays from electroweak fits [22] and the exclusion from low energy measurements [23].

4.2 Charginos and neutralinos decaying via $LL\bar{E}$

Depending on the masses of the gauginos and on the lepton flavour composition in the decay, the indirect decays of charginos to neutralinos and of heavier neutralinos to lighter neutralinos populate different regions in track multiplicity, visible mass and leptonic energy. For this reason three different subselections were developed [4], covering topologies with large leptonic energies and at least two jets (Subselection I), topologies with small multiplicities and large leptonic energy fractions (Subselection II), and topologies with a moderate leptonic energy fraction (Subselection III). The combination of the three subselections is defined as the “Leptons and Hadrons” selection. The complete set of cuts, updated for $\sqrt{s} > 184 \text{ GeV}$ is shown in Table 3.

**Fig. 5a–d.** The 95% C.L. limits in the $(M_\chi, M_{\tilde{t}_1})$ and $(M_\chi, M_{\tilde{b}_1})$ planes for indirect decays via the $LL\bar{E}$ couplings λ_{122} and λ_{133} are shown for no mixing ($\phi_{\text{mix}} = 0^\circ$) and for $\phi_{\text{mix}} = 56^\circ, 66^\circ$ for stops and sbottoms, respectively. The LEP 2 exclusion corresponds to the absolute limit on M_χ

Interpreting the results, shown in Table 2, in the framework of the MSSM, 95% C.L. exclusion limits are derived in the (μ, M_2) plane and shown in Fig. 4a for large scalar masses $m_0 = 500 \text{ GeV}/c^2$. The corresponding lower limit on the mass of the lightest chargino is essentially at the kinematic limit for pair production.

The searches for the lightest and second lightest neutralino do not extend the excluded region in the (μ, M_2) plane beyond that achieved with the chargino search alone.

4.3 Squarks decaying via $LL\bar{E}$

Although squarks cannot decay directly with an $LL\bar{E}$ coupling, they may decay indirectly to the lightest neutralino. This topology is searched for by means of the “Leptons and Hadrons” selection. The 95% C.L. squark mass limits

Table 3. The list of cuts for the “Leptons and Hadrons” selection, which is used for charginos and squarks decaying indirectly via the $LL\bar{E}$ operator. The event variables are defined in [4]

Subselection I	Subselection II	Subselection III
$N_{\text{ch}} \geq 5$	$5 \leq N_{\text{ch}} \leq 15$	$N_{\text{ch}} \geq 11$
$M_{\text{vis}} > 25 \text{ GeV}/c^2$	$20 \text{ GeV}/c^2 < M_{\text{vis}} < 75\%\sqrt{s}$	$55\%\sqrt{s} < M_{\text{vis}} < 80\%\sqrt{s}$
$p_{\perp}^{\text{miss}} > 3.5\%\sqrt{s}$	$p_{\perp}^{\text{miss}} > 2.5\%\sqrt{s}$	$p_{\perp}^{\text{miss}} > 5\%\sqrt{s}$
$ p_z^{\text{miss}} < 20 \text{ GeV}/c$		$N_{\text{ch}}^{\text{jet}} \geq 1$
	$y_3 > 0.009$	$y_3 > 0.025$
	$y_4 > 0.0026$	$y_4 > 0.012$
$y_5 > 0.006$		$y_5 > 0.004$
		$T < 0.85$
$N_{\text{lep}} \geq 1$	$N_{\text{lep}} \geq 1$	$N_{\text{lep}} \geq 1$
$E_{\text{nonlep}} < 50\%\sqrt{s}$	$E_{\text{nonlep}} < 50\%\sqrt{s}$	
$E_{\text{had}} < 28\%E_{\text{vis}}$	$E_{\text{had}} < 22\%E_{\text{lep}}$	$E_{\text{lep}} > 20\%E_{\text{had}}$
	$\chi_{\text{WW}}^2 > 3.8$	

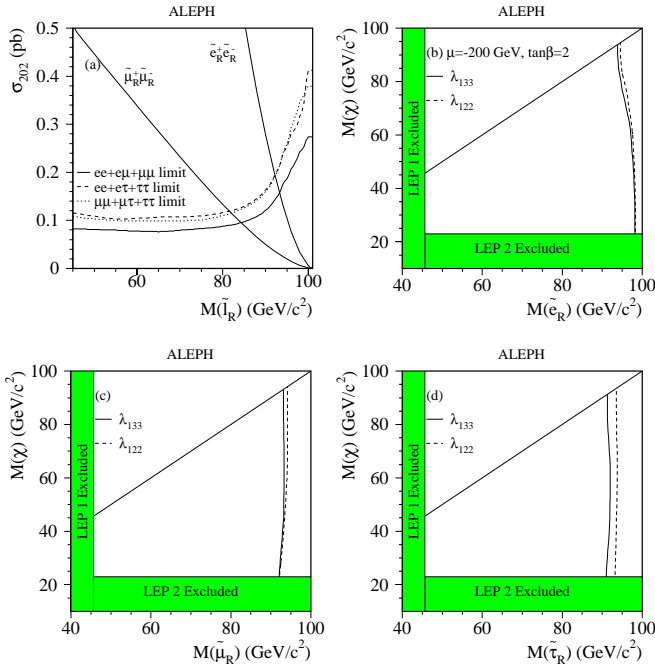


Fig. 6. **a** The 95% C.L. exclusion cross sections for sleptons decaying directly via a dominant $LL\bar{E}$ operator. The MSSM cross section for pair production of right-handed selectrons and smuons are superimposed. **b–d** show the 95% C.L. limits in the $(M_\chi, M_{\tilde{l}_R})$ plane for indirect decays of selectrons, smuons and staus, respectively. The two choices of λ_{122} and λ_{133} correspond to the best and worst case exclusions, respectively. The selectron cross section is evaluated at $\mu = -200 \text{ GeV}/c^2$ and $\tan\beta = 2$

are presented as functions of M_χ in Fig. 5 for the case of \tilde{t}_1 and \tilde{b}_1 squarks. The following limits upon the right-handed squarks can be derived: $M_{\tilde{u}_R} > 90 \text{ GeV}/c^2$ and $M_{\tilde{d}_R} > 89 \text{ GeV}/c^2$ for any λ_{ijk} .

4.4 Sleptons decaying via $LL\bar{E}$

A right-handed slepton can decay directly via the $LL\bar{E}$ coupling to a lepton and anti-neutrino, hence the acoplanar lepton selection is used. For a given choice of generation indices the decay will produce two final states equally; for the coupling λ_{ijk} these decays are $\tilde{l}_R^k \rightarrow l^i \bar{\nu}_{l_j}$ or $\bar{\nu}_{l_i} l^j$. Excluded cross sections are shown in Fig. 6a for the different mixtures of acoplanar lepton states. The MSSM production cross section for right-handed smuon pairs and selectron pairs at $\mu = -200 \text{ GeV}/c^2$ and $\tan\beta = 2$ are superimposed. The cross section limit translates into a lower bound on the smuon (or stau) mass of $M_{\tilde{\mu}_R, \tilde{\tau}_R} > 81 \text{ GeV}/c^2$ and $M_{\tilde{e}_R} > 92 \text{ GeV}/c^2$ ($\mu = -200 \text{ GeV}/c^2$, $\tan\beta = 2$) for the direct decays and the worst case coupling.

Indirect decays of sleptons are selected using the “Six Leptons + \bar{E} ” selection. Limits corresponding to this case are shown in Fig. 6b–d. Using the bound of $M_\chi > 23 \text{ GeV}/c^2$ these limits can be interpreted as the mass limits $M_{\tilde{e}_R} > 93 \text{ GeV}/c^2$ ($\mu = -200 \text{ GeV}/c^2$, $\tan\beta = 2$), $M_{\tilde{\mu}_R} > 92 \text{ GeV}/c^2$ and $M_{\tilde{\tau}_R} > 91 \text{ GeV}/c^2$ for the worst case coupling.

4.5 Sneutrinos decaying via $LL\bar{E}$

In pair production each sneutrino can decay directly into pairs of charged leptons giving the final states $eeee$, $ee\mu\mu$, $ee\tau\tau$, $\mu\mu\mu\mu$, $\mu\mu\tau\tau$ and $\tau\tau\tau\tau$. The different final states correspond to different choices of generation indices. The “Four Lepton” selection was used to derive exclusion limits on the sneutrino pair production cross section shown in Fig. 7a. These limits translate into a lower bound on the electron sneutrino mass of $M_{\tilde{\nu}_e} > 98 \text{ GeV}/c^2$ ($\mu = -200 \text{ GeV}/c^2$, $\tan\beta = 2$) and the muon sneutrino mass of $M_{\tilde{\nu}_\mu} > 86 \text{ GeV}/c^2$ for direct decays and the worst case coupling.

Table 4. The observed numbers of events in the data and the Standard Model background expectations for the $LQ\bar{D}$ selections

\sqrt{s} (GeV)	188.6		191.6		195.5		199.5		201.6		All	
Selection	Data	SM	Data	SM	Data	SM	Data	SM	Data	SM	Data	SM
MultiJets + Leptons	13	11	1	1.8	6	4.7	3	5.2	5	2.6	28	26
Jets-HM	11	8.7	1	1.3	3	3.1	1	2.8	3	1.3	19	17
4 Jets + 2τ	10	13	2	2.0	1	5.1	7	5.3	5	2.7	25	28
Four-Jets	684	754	143	127	322	351	336	370	147	179	1632	1780
2 Jets + 2τ	10	11	1	1.9	5	5.8	6	5.2	3	2.5	25	26
AJ-H	10	12	2	2.2	9	6.8	7	8.6	10	4.6	38	34
4JH	5	7.8	1	1.3	3	3.7	0	3.9	4	2.0	13	19
5 Jets + 1 Iso. l	4	4.2	1	0.7	1	1.9	0	1.9	0	0.9	6	9.6
4 Jets + 2 Iso. l	0	3.1	0	0.5	1	1.3	3	1.5	1	0.7	5	7.1

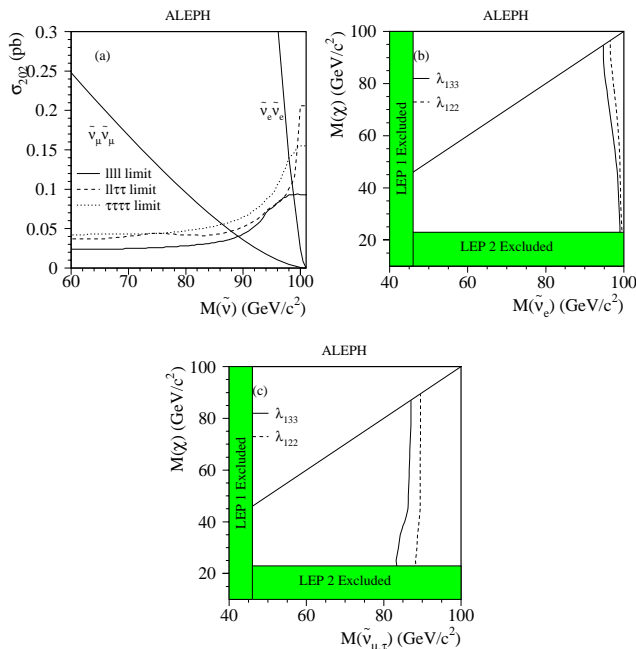


Fig. 7. **a** The 95% C.L. exclusion cross sections for sneutrinos decaying directly via a dominant $LL\bar{E}$ operator. The three curves correspond to different possible final states, with $l=e$ or μ , due to the specific choice of sneutrino flavour and λ_{ijk} . The MSSM cross section for pair production of muon and electron sneutrinos are superimposed; the tau sneutrinos have the same cross section as the muon type. **b** shows the 95% C.L. limits in the $(M_\chi, M_{\tilde{\nu}_e})$ plane for $\tilde{\nu}_e$, and figure **c** for both $\tilde{\nu}_\mu$ and $\tilde{\nu}_\tau$ indirect decays. The two choices of λ_{122} and λ_{133} correspond to the best and worst case exclusions, respectively. The electron sneutrino cross section is evaluated at $\mu = -200 \text{ GeV}/c^2$ and $\tan\beta = 2$

Indirect decays of sneutrinos are selected using the “Four Leptons + \cancel{E} ” selection. The limits in the $(M_\chi, M_{\tilde{\nu}})$ plane corresponding to this case are shown in Fig. 7b and c. Using the bound $M_\chi > 23 \text{ GeV}/c^2$ this limit can be interpreted as $M_{\tilde{\nu}_{\mu,\tau}} > 83 \text{ GeV}/c^2$ and $M_{\tilde{\nu}_e} > 94 \text{ GeV}/c^2$

for the worst case coupling, where the cross section for the electron sneutrino is evaluated at $\mu = -200 \text{ GeV}/c^2$ and $\tan\beta = 2$.

5 Decays via a dominant $LQ\bar{D}$ Coupling

For a dominant $LQ\bar{D}$ operator the event topologies are mainly characterised by large hadronic activity, possibly with some leptons and/or missing energy. In the simplest case the topology consists of four-jet final states, and in more complicated scenarios of multi-jet and multi-lepton and/or multi-neutrino states. A summary of the results of the various selections is given in Table 4.

The acoplanar jet selection (AJ-H) and the four jets and missing energy selection (4JH) developed for R-parity conserving SUSY searches are used [24]. The “MultiJets + Leptons” and the “ $2J+2\tau$ ” selections are updated from [4] and reoptimised for the higher centre-of-mass energy as described below. The “4 Jets + 2τ ” is unchanged from [25]. Two new selections for five jets and one isolated lepton and four jets and two isolated leptons, “5 Jets + 1 Iso. l ” and “4 Jets + 2 Iso. l ”, are described below.

5.1 Charginos and neutralinos decaying via $LQ\bar{D}$

Three subselections were developed to select the chargino indirect topologies [4]; some cuts have been reoptimised for the higher centre-of-mass energy. Subselection I is designed to select final states based on hadronic activity, e.g. $\chi^+\chi^- \rightarrow qq\bar{q}\bar{q}\chi\chi$; subselection II is designed for decays such as $\chi^+\chi^- \rightarrow lvqq\chi\chi$ where the leptonic energy is larger, and subselection III is designed to select the decays $\chi^+\chi^- \rightarrow lvlv\chi\chi$. The combination of the three subselections is defined as the “Multi-jets plus Leptons” selection. The complete set of cuts is shown in Table 5.

Interpreting these results in the framework of the MSSM, 95% C.L. exclusion limits are derived in the (μ, M_2) plane and shown in Fig. 4b for large scalar masses

Table 5. The list of cuts for the “Multi-jets plus Leptons” selection used to select indirect chargino decays via the $LQ\bar{D}$ operator. The “Jets-HM” selection is also listed; this is used to select intermediate ΔM indirect squark decays with high visible mass. Primed event variables are calculated from physical quantities excluding identified leptons. The event variables are defined in [4]

Subselection I	Subselection II	Subselection III	Jets-HM
	$N_{\text{ch}} \geq 10$		$N_{\text{ch}} \geq 30$
	$M_{\text{vis}} > 45 \text{ GeV}/c^2$		$M_{\text{vis}} > 100 \text{ GeV}/c^2$
	$\Theta_{\text{miss}} > 30^\circ$		$\Theta_{\text{miss}} > 30^\circ$
$M'_{\text{vis}} > 50\%\sqrt{s}$	$M'_{\text{vis}} < 50\%\sqrt{s}$	$M'_{\text{vis}} < 65 \text{ GeV}/c^2$	$M'_{\text{vis}} > 50\%\sqrt{s}$
$T < 0.9$	$T < 0.74$	$T < 0.8$	$T < 0.85$
	$y'_4 > 0.0047$	$y'_4 > 0.001$	
$y_5 > 0.003$	$\left(\begin{array}{c} \Phi'_{\text{aco}} < 145^\circ \\ \text{or} \\ y_6 > 0.002 \end{array} \right)$		$y_5 > 0.003$
$y_6 > 0.002$		$y_6 > 0.00035$	$y_6 > 0.002$
$E_T > 80 \text{ GeV}$			$E_T > 80 \text{ GeV}$
$E_{\text{jet}}^{\text{em}} < 90\%E_{\text{jet}}$	$E_{\text{lep}} < 40 \text{ GeV}$		$E_{\text{jet}}^{\text{em}} < 85\%E_{\text{jet}}$
$E_{10}^{\text{iso}} < 5 \text{ GeV}$	$E_{\text{had}} < 2.5E_{\text{lep}}$	$E_{\text{had}} < 47\%E_{\text{lep}}$	$E_{10}^{\text{iso}} < 5 \text{ GeV}$
$[0.55(M'_{\text{vis}} - 120) + \Phi'_{\text{aco}}] < 180^\circ$	$\chi^2_{\text{WW}} > 3.8$		$[0.55(M'_{\text{vis}} - 120) + \Phi'_{\text{aco}}] < 190^\circ$

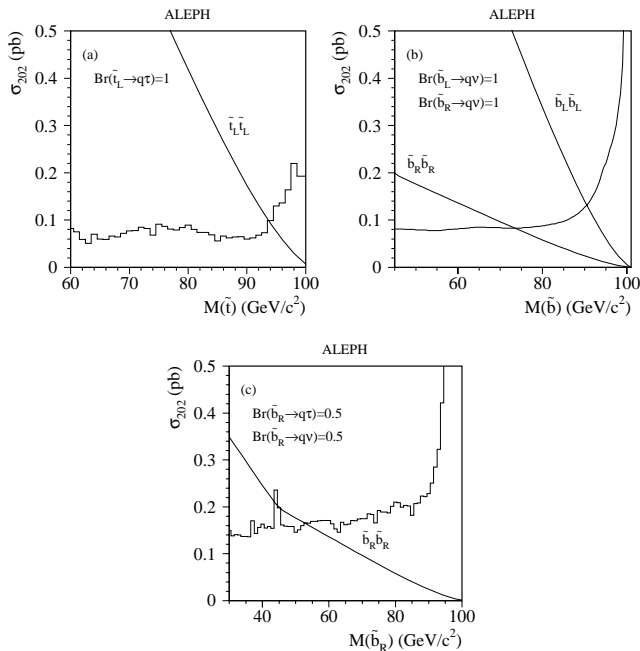


Fig. 8a–c. The 95% C.L. excluded cross sections for the production of squarks decaying directly via a dominant $LQ\bar{D}$ operator: **a** \tilde{t}_L (λ'_{33k}), **b** \tilde{b}_L (λ'_{3k}) or \tilde{b}_R (λ'_{33}), and **c** \tilde{b}_R (λ'_{3j3}). The MSSM cross sections are superimposed

($m_0 = 500 \text{ GeV}/c^2$). The corresponding lower limit on the mass of the lightest chargino is essentially at the kinematic limit for pair production.

The searches for the lightest and second lightest neutralino do not extend the excluded region in the (μ, M_2) plane beyond that achieved with the chargino search alone.

5.2 Squarks decaying via $LQ\bar{D}$

A squark can decay directly to a quark and either a lepton or a neutrino leading to topologies with acoplanar jets and up to two leptons. Couplings with electrons or muons in the final state are not considered as existing limits from the Tevatron [26] exclude the possibility of seeing such a signal at LEP. To select $\tilde{q} \rightarrow q\tau$ and $\tilde{q} \rightarrow q\nu$, the “2J+2 τ ” and the “AJ-H” selections are used. The “2J+2 τ ” selection is unchanged from [4] except that the sliding mass window is now $10 \text{ GeV}/c^2$ wide centred on the squark mass. Examples of limits for squark production are shown in Fig. 8. In particular, for a dominant λ'_{33k} coupling, which implies $\text{Br}(\tilde{t}_L \rightarrow q\tau) = 100\%$, a lower limit of $93 \text{ GeV}/c^2$ is obtained for $M_{\tilde{t}_L}$.

Indirect decays of squarks via the $LQ\bar{D}$ operator will give six jets and up to two charged leptons. These are selected by the “4 Jets + 2 τ ” selection if $M_\chi \leq 20 \text{ GeV}/c^2$, either the “5 Jets + 1 Iso. l ” or “Multi-jets plus Leptons” if $(M_{\tilde{q}} - M_\chi) \leq 15 \text{ GeV}/c^2$, otherwise the “Jets-HM” selection is used. The cuts used for the “5 Jets + 1 Iso. l ” selection are listed in Table 6. Limits for the optimistic case of left-handed squarks are shown in Fig. 9. The following limits for \tilde{t}_L and \tilde{b}_L are derived: $M_{\tilde{t}_L} > 84 \text{ GeV}/c^2$ and $M_{\tilde{b}_L} > 74 \text{ GeV}/c^2$.

5.3 Sleptons and sneutrinos decaying via $LQ\bar{D}$

Direct decays of sleptons and sneutrinos via the $LQ\bar{D}$ operator lead to four jet final states. The “Four-Jets” selection from [4] is applied. The distributions of the di-jet masses for data and Monte Carlo are shown in Fig. 10a. Fewer events are observed around the W mass peak region

Table 6. The list of cuts for the “5 Jets + 1 Isolated Leptons” and “4 Jets + 2 Isolated Leptons” selections, as used for the indirect squark and slepton searches decaying via an $LQ\bar{D}$ operator. M''_{vis} is the visible mass after the two leading leptons are removed. Other variables are defined in [4]

5 Jets + 1 Iso. l	4 Jets + 2 Iso. l
$N_{ch} > 9$	$N_{ch} > 9$
$E_{vis} < 95\%\sqrt{s}$	$E_{vis} > 65\%\sqrt{s}$
$N_{lep} \geq 1$	$N_{lep} \geq 2$ (same flavour e or μ)
$p_{\perp}^{miss} > 5 \text{ GeV}/c$	
$\Theta_{miss} > 18^\circ$	
$E_{l_1} > 10 \text{ GeV}$	$E_{l_1} > 5 \text{ GeV}, E_{l_2} > 5 \text{ GeV}$
$E_{l_1}^{iso} < 5 \text{ GeV}$	$E_{l_1}^{iso} < 5 \text{ GeV}, E_{l_2}^{iso} < 5 \text{ GeV}$
$y_5 > 0.003$	$y_5 > 0.001$
$y_6 > 0.001$	$y_6 > 0.0005$
$\min\{ M_{vis} - 91.2 , M''_{vis} - 91.2 \} > 3 \text{ GeV}/c^2$	$ M''_{vis} - 91.2 > 5 \text{ GeV}/c^2$
$\chi_{WW}^2 > 3.8$	

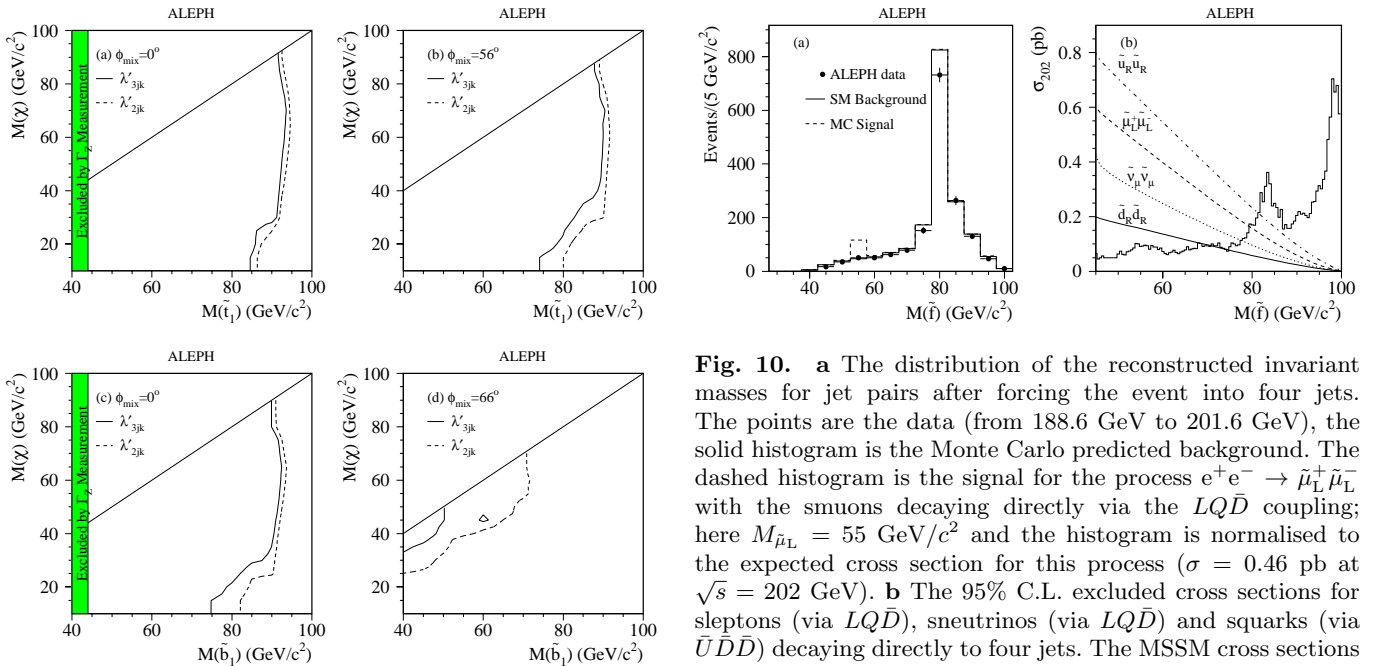


Fig. 9a–d. The 95% C.L. limits in the $(M_\chi, M_{\tilde{t}_1})$ and $(M_\chi, M_{\tilde{b}_1})$ planes for indirect $LQ\bar{D}$ decays via the λ'_{211} and λ'_{311} couplings, for no squark mixing ($\phi_{mix} = 0^\circ$) and for $\phi_{mix} = 56^\circ, 66^\circ$ for stops and sbottoms, respectively

than expected. Limits are derived by sliding a mass window of $5 \text{ GeV}/c^2$ across the di-jet mass distribution. The results are shown in Fig. 10b and imply $M_{\tilde{\nu}_\mu} > 77 \text{ GeV}/c^2$ and $M_{\tilde{\mu}_L} > 79 \text{ GeV}/c^2$.

Indirect decays of the sleptons via the $LQ\bar{D}$ operator will give two, three or four leptons and four jets in the final state; two leptons will be of the same flavour as the initial sleptons. The indirect decays of sneutrinos will give a final state with four jets, up to two leptons and missing

Fig. 10. **a** The distribution of the reconstructed invariant masses for jet pairs after forcing the event into four jets. The points are the data (from 188.6 GeV to 201.6 GeV), the solid histogram is the Monte Carlo predicted background. The dashed histogram is the signal for the process $e^+e^- \rightarrow \tilde{\mu}_L^+ \tilde{\mu}_L^-$ with the smuons decaying directly via the $LQ\bar{D}$ coupling; here $M_{\tilde{\mu}_L} = 55 \text{ GeV}/c^2$ and the histogram is normalised to the expected cross section for this process ($\sigma = 0.46 \text{ pb}$ at $\sqrt{s} = 202 \text{ GeV}$). **b** The 95% C.L. excluded cross sections for sleptons (via $LQ\bar{D}$), sneutrinos (via $LQ\bar{D}$) and squarks (via $U\bar{D}\bar{D}$) decaying directly to four jets. The MSSM cross sections for pair production of muon sneutrinos, left-handed smuons and right-handed squarks are superimposed

energy. For selectrons and smuons the “4 Jets + 2 Iso. l ” selection is used except for the special case of $\lambda'_{3jk} \neq 0$ and $(M_{\tilde{l}_R} - M_\chi) < 10 \text{ GeV}/c^2$ where the “4 Jets + 2τ ” selection is used. The cuts used in the “4 Jets + 2 Iso. l ” are listed in Table 6. Indirect stau decays are selected with the “5 Jets + 1 Iso. l ” selection if $M_\chi > 20 \text{ GeV}/c^2$ and either $\lambda'_{2jk} \neq 0$ or $\lambda'_{1jk} \neq 0$, otherwise the inclusive combination of the “5 Jets + 1 Iso. l ” and the “Leptons and Hadrons” selections is used. The sneutrinos are selected with the “4JH” selection for $M_\chi > 20 \text{ GeV}/c^2$ and “AJ-H” (acoplanar jets) otherwise. Limits for these decays are shown in Fig. 11 and Fig. 12. The limits are $M_{\tilde{e}_R} > 89 \text{ GeV}/c^2$,

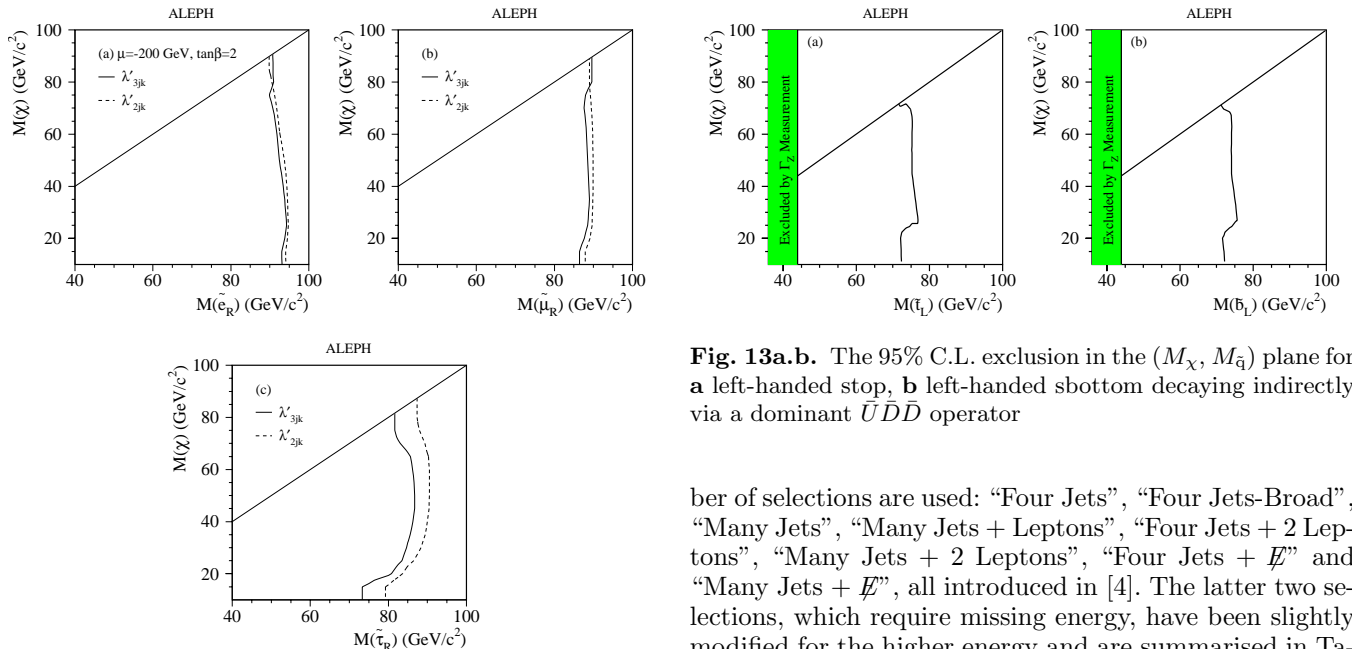


Fig. 11a–c. The 95% C.L. limits in the $(M_\chi, M_{\tilde{q}_R})$ plane for selectrons, smuons and staus decaying indirectly via a dominant $LQ\bar{D}$ operator. The two choices of λ'_{2jk} and λ'_{3jk} correspond to the best and worst case exclusions, respectively. The selectron cross section is evaluated at $\mu = -200 \text{ GeV}/c^2$ and $\tan\beta = 2$. The limit from the Γ_Z measurements excludes $M_{\tilde{q}} < 38 \text{ GeV}/c^2$

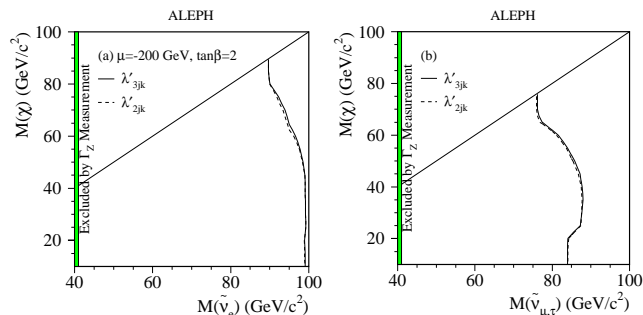


Fig. 12a.b. The 95% C.L. limits in the $(M_\chi, M_{\tilde{\nu}})$ plane for electron and muon or tau sneutrinos decaying indirectly via a dominant $LQ\bar{D}$ operator. The two choices of λ'_{2jk} and λ'_{3jk} correspond to the best and worst case exclusions, respectively. The electron sneutrino cross section is evaluated at $\mu = -200 \text{ GeV}/c^2$ and $\tan\beta = 2$

$M_{\tilde{\mu}_R} > 86 \text{ GeV}/c^2$, $M_{\tilde{\tau}_R} > 73 \text{ GeV}/c^2$, $M_{\tilde{\nu}_e} > 89 \text{ GeV}/c^2$ and $M_{\tilde{\nu}_\mu} > 75 \text{ GeV}/c^2$ for the worst case couplings; the selectron and electron sneutrino cross sections are evaluated at $\mu = -200 \text{ GeV}/c^2$ and $\tan\beta = 2$.

6 Decays via a dominant $\bar{U}\bar{D}\bar{D}$ coupling

For a dominant $\bar{U}\bar{D}\bar{D}$ operator the final states are characterised by topologies having many hadronic jets, possibly associated with leptons and missing energy. A num-

Fig. 13a.b. The 95% C.L. exclusion in the $(M_\chi, M_{\tilde{q}})$ plane for **a** left-handed stop, **b** left-handed sbottom decaying indirectly via a dominant $\bar{U}\bar{D}\bar{D}$ operator

ber of selections are used: “Four Jets”, “Four Jets-Broad”, “Many Jets”, “Many Jets + Leptons”, “Four Jets + 2 Leptons”, “Many Jets + 2 Leptons”, “Four Jets + \cancel{E} ” and “Many Jets + \cancel{E} ”, all introduced in [4]. The latter two selections, which require missing energy, have been slightly modified for the higher energy and are summarised in Table 7. These selections rely mainly on two characteristics of the events: mass reconstruction of the pair produced sparticles and/or the presence of many jets in the event. Table 8 gives a list of all the selections and the numbers of observed and expected events.

6.1 Charginos and neutralinos decaying via $\bar{U}\bar{D}\bar{D}$

The decay of the lightest neutralino and direct decays of the chargino both lead to six hadronic jets in the final state. The indirect chargino decays give rise to a variety of final states depending on the W^* decay, they range from ten hadronic jets to six jets associated with leptons and missing energy. The “Many Jets”, “Four Jets” and “Many Jets + Lepton” selections are used to cover these topologies.

Interpreting these results in the framework of the MSSM, Fig. 4c shows the 95% C.L. exclusion in the (μ, M_2) plane. As for the LLE and $LQ\bar{D}$ couplings the lower limit on the lightest chargino mass is essentially at the kinematic limit.

The searches for the lightest and second lightest neutralino do not extend the excluded region in the (μ, M_2) plane beyond that achieved with the chargino search alone.

6.2 Squarks decaying via $\bar{U}\bar{D}\bar{D}$

The direct decay of pair produced squarks leads to four-quark final states. The “Four Jet” selection is therefore used to extract the mass limits. As shown in Fig. 10b the mass limits are $82 \text{ GeV}/c^2$ for up-type squarks and $68 \text{ GeV}/c^2$ for down-type squarks.

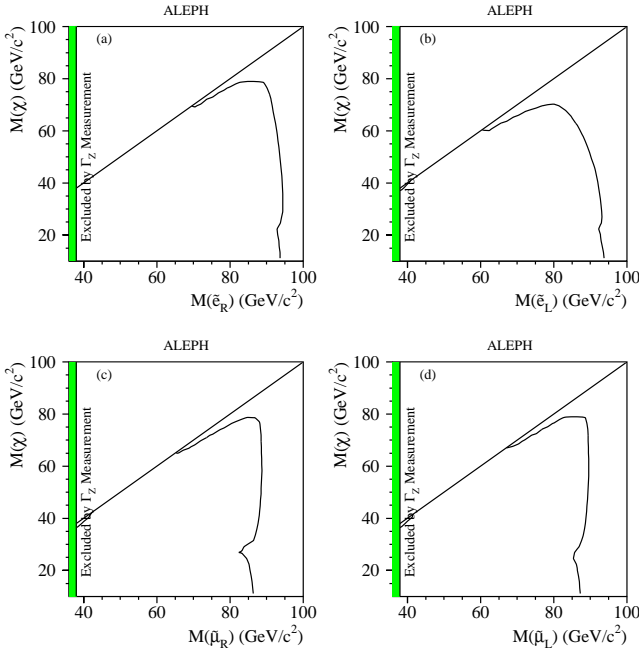
For the indirect squark decays, which lead to eight-jet topologies, the “Four Jets-Broad” selection is used. The resulting 95% C.L. exclusion in the $(M_\chi, M_{\tilde{q}})$ plane for left-handed stop and sbottom are shown in Fig. 13. The

Table 7. The list of cuts for the “Four Jets + \cancel{E} ” and “Many Jets + \cancel{E} ” selections, as used for the indirect sneutrino searches via a $\bar{U}\bar{D}\bar{D}$ operator

Four Jets + \cancel{E}	Many Jets + \cancel{E}
$N_{\text{ch}} > 8$	
$ p_z^{\text{miss}} /p^{\text{miss}} < 0.95$	
$E_{\text{jet}}^{\text{em}} < 95\%E_{\text{jet}}, E_T > 60 \text{ GeV}, E_{\text{lep}} < 15 \text{ GeV}$	
$0.25 < E_{\text{vis}}/\sqrt{s} < 0.75$	$0.5 < E_{\text{vis}}/\sqrt{s} < 0.95$
$\Delta\phi_T < 170^\circ$	
$0.5 < T < 0.97$	$0.6 < T < 0.97$
$y_4 > 0.001$	$y_4 > 0.005$
$y_6 > 0.0003$	$y_6 > 0.002$ (0.005 if $M_\chi > 60 \text{ GeV}$)
$ M_{12-34} < 10 \text{ GeV}/c^2$ if $M_\chi < 60 \text{ GeV}/c^2$: $ M_{12-34} < 10 \text{ GeV}/c^2$	
$ M_{12+34} - 2M_\chi < M_\chi/3$ if $M_\chi < 60 \text{ GeV}/c^2$: $ M_{12+34} - 2M_\chi < M_\chi/3$	

Table 8. The observed numbers of events in the data and the corresponding Standard Model background expectations for the $\bar{U}\bar{D}\bar{D}$ selections, quoted with any sliding mass cuts removed

\sqrt{s} (GeV)	188.6		191.6		195.5		199.5		201.6		All	
	Data	SM	Data	SM	Data	SM	Data	SM	Data	SM	Data	SM
Four Jets Broad	126	133	19	22	57	57	61	60	23	29	286	299
Many Jets	10	10	1	1.6	6	4.4	8	4.2	3	2.0	28	22
Many Jets + Leptons	22	17	3	2.9	8	7.0	10	7.8	9	3.8	52	39
Four Jets + 2 Leptons	6	4.0	1	0.98	0	2.2	5	2.5	2	1.2	14	11
Many Jets + 2 Leptons	6	6.5	2	1.4	2	2.8	2	4.0	3	1.9	15	17
Four Jets + \cancel{E}	68	77	15	14	35	34	40	37	20	18	178	175
Many Jets + \cancel{E}	87	80	17	14	50	34	38	36	18	17	210	179

**Fig. 14a–d.** The 95% C.L. excluded cross sections for left or right-handed selectrons and smuons decaying indirectly via a dominant $\bar{U}\bar{D}\bar{D}$ operator. The selectron cross section is evaluated in the region $\mu = -200 \text{ GeV}/c^2$ and $\tan\beta = 2$

corresponding mass limits are $M_{\tilde{t}_L} > 71.5 \text{ GeV}/c^2$ and $M_{\tilde{b}_L} > 71.5 \text{ GeV}/c^2$.

6.3 Sleptons decaying via $\bar{U}\bar{D}\bar{D}$

No direct slepton decays are possible via the $\bar{U}\bar{D}\bar{D}$ coupling. For the indirect decays of selectron and smuon pairs, which lead to six-jets plus two-lepton final states, the “Four Jets + 2 Leptons” selection is used for large mass differences between the slepton and neutralino, and the “Many Jets + 2 Leptons” for the low mass difference region. In addition, for the very low mass difference region the leptons are very soft and the “Four Jets” selection is used.

Figure 14 shows the 95% C.L. exclusion in the $(M_\chi, M_{\tilde{\ell}})$ plane for selectrons and smuons. The selectron cross section is evaluated at $\mu = -200 \text{ GeV}/c^2$ and $\tan\beta = 2$. The shape of the limits at $M_\chi \approx 20 \text{ GeV}/c^2$ is due to the switch between selections. For $M_{\tilde{\ell}} - M_\chi > 10 \text{ GeV}/c^2$ this yields $M_{\tilde{e}_R} > 88.5 \text{ GeV}/c^2$ and $M_{\tilde{\mu}_R} > 82.5 \text{ GeV}/c^2$.

6.4 Sneutrinos decaying via $\bar{U}\bar{D}\bar{D}$

No direct sneutrino decays are possible via the $\bar{U}\bar{D}\bar{D}$ coupling. Sneutrinos decaying indirectly lead to six-jet final

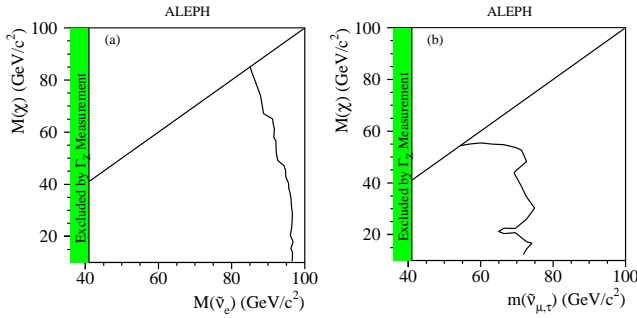


Fig. 15. **a** The 95% C.L. exclusion in the $(M_\chi, M_{\tilde{\nu}_e})$ plane for $\tilde{\nu}_e$ decaying indirectly via a dominant $\bar{U}\bar{D}\bar{D}$ operator. The $\tilde{\nu}_e$ cross section is evaluated at $\mu = -200 \text{ GeV}/c^2$ and $\tan\beta = 2$. **b** The exclusion obtained in the $(M_\chi, M_{\tilde{\nu}_{\mu,\tau}})$ plane for $\tilde{\nu}_{\mu,\tau}$ decaying indirectly via a dominant $\bar{U}\bar{D}\bar{D}$ operator

states containing two neutrinos. Large mass differences between the sneutrino and neutralino lead to event topologies with significant missing energy, and the “Four Jets + \cancel{E} ” selection is used. For small mass differences the “Many Jets + \cancel{E} ” selection is used.

Figure 15 shows the 95% C.L. exclusion in the $(M_\chi, M_{\tilde{\nu}})$ plane for the electron sneutrino (Fig. 15a) and muon or tau sneutrino (Fig. 15b). The electron sneutrino cross sections is evaluated at $\mu = -200 \text{ GeV}/c^2$ and $\tan\beta = 2$. The limits $M_{\tilde{\nu}_e} > 84 \text{ GeV}/c^2$ and $M_{\tilde{\nu}_{\mu,\tau}} > 64 \text{ GeV}/c^2$ are obtained.

7 Summary

A number of searches were developed to select R-parity violating decay topologies for single and pair production of SUSY particles. It has been assumed that the LSP has a negligible lifetime, and that only one coupling $\lambda_{ijk}, \lambda'_{ijk}$ or λ''_{ijk} is nonzero. These searches found no evidence for R-parity violating supersymmetry in the data collected at $\sqrt{s} = 188.6\text{--}201.6 \text{ GeV}$, and various limits were set within the framework of the MSSM.

From searches for singly produced sneutrinos, upper limits on the values of the λ_{121} and λ_{131} couplings were set as a function of $M_{\tilde{\nu}_\mu}$ and $M_{\tilde{\nu}_\tau}$, respectively.

The limits for direct decays of sleptons for an $LL\bar{E}$ coupling are $M_{\tilde{e}_R} > 92 \text{ GeV}/c^2$ and $M_{\tilde{\nu}_e} > 98 \text{ GeV}/c^2$ at $\mu = -200 \text{ GeV}/c^2$ and $\tan\beta = 2$, $M_{\tilde{\mu}_R, \tilde{\tau}_R} > 81 \text{ GeV}/c^2$ and $M_{\tilde{\nu}_{\mu,\tau}} > 86 \text{ GeV}/c^2$. The limits for the direct decays of sleptons and squarks in the case of an $LQ\bar{D}$ coupling are $M_{\tilde{\mu}_L} > 79 \text{ GeV}/c^2$, $M_{\tilde{\nu}_\mu} > 77 \text{ GeV}/c^2$ and $M_{\tilde{t}_L} > 93 \text{ GeV}/c^2$ for $\text{Br}(\tilde{t}_L \rightarrow q\tau) = 1$. The limit for squarks assuming a $\bar{U}\bar{D}\bar{D}$ coupling are $M_{\tilde{u}_R} > 82 \text{ GeV}/c^2$ and $M_{\tilde{d}_R} > 68 \text{ GeV}/c^2$.

For the indirect decays of sfermions, the limits listed in Table 9 have been obtained, assuming $M_{\tilde{\ell}} - M_\chi > 10 \text{ GeV}/c^2$ for $LQ\bar{D}$ and $\bar{U}\bar{D}\bar{D}$, $M_\chi > 23 \text{ GeV}/c^2$ for $LL\bar{E}$ and derived at $\mu = -200 \text{ GeV}/c^2$ and $\tan\beta = 2$ for \tilde{e} and $\tilde{\nu}_e$.

Table 9. The 95% confidence level lower mass limits for sparticles decaying indirectly for each of the three R-parity violating couplings

Sparticle	Lower mass limit (GeV/c^2)		
	$LL\bar{E}$	$LQ\bar{D}$	$\bar{U}\bar{D}\bar{D}$
\tilde{t}_1	90	84	71.5
\tilde{b}_1	89	74	71.5
\tilde{e}_R	93	89	88.5
$\tilde{\mu}_R$	92	86	82.5
$\tilde{\tau}_R$	91	73	×
$\tilde{\nu}_e$	94	89	84
$\tilde{\nu}_{\mu,\tau}$	83	75	64

Assuming large m_0 the chargino mass limit is given by the kinematic limit $M_{\chi^+} > 100 \text{ GeV}/c^2$, irrespective of the R-parity violating operator.

Acknowledgements. It is a pleasure to congratulate our colleagues from the accelerator divisions for the successful operation of LEP at high energy. We would like to express our gratitude to the engineers and support people at our home institutes without whose dedicated help this work would not have been possible. Those of us from non-member states wish to thank CERN for its hospitality and support.

References

- For a review see for example H.P. Nilles, Phys. Rep. **110** (1984) 1; H. E. Haber, G. L. Kane, Phys. Rep. **117** (1985) 75
- G. Farrar, P. Fayet, Phys. Lett. **B 76** (1978) 575
- S. Weinberg, Phys. Rev. **D 26** (1982) 287; N. Sakai, T. Yanagida Nucl. Phys. **B 197** (1982) 83; S. Dimopoulos, S. Raby, F. Wilczek, Phys. Lett. **B 212** (1982) 133
- ALEPH Collaboration, “Search for R-parity violating decays of supersymmetric particles in e^+e^- collisions at centre-of-mass energies near 183 GeV”, Eur. Phys. J. **C13** (2000) 29
- DELPHI Collaboration, “Search for supersymmetry with R-parity violating $LL\bar{E}$ couplings at $\sqrt{s} = 183 \text{ GeV}$ ”, Eur. Phys. J. **C13** (2000) 591
- OPAL Collaboration, “Searches for R-Parity violating decays of Gauginos at 183 GeV at LEP”, Eur. Phys. J. **C11** (1999) 619
- OPAL Collaboration, “Search for R-parity Violating Decays of Scalar Fermions at LEP”, Eur. Phys. J. **C12** (2000) 1
- L3 Collaboration, “Search for R-Parity Breaking Sneutrino Exchange at LEP”, Phys. Lett. **B 414** (1997) 373
- L3 Collaboration, “Search for R-parity Violating Chargino and Neutralino Decays in e^+e^- Collisions up to $\sqrt{s} = 183 \text{ GeV}$ ”, Phys. Lett. **B 459** (1999) 354
- ALEPH Collaboration, “ALEPH: a detector for electron-positron annihilations at LEP”, Nucl. Instr. Meth. **A 294** (1990) 121
- ALEPH Collaboration, “Performance of the ALEPH detector at LEP”, Nucl. Instr. Meth. **A 360** (1995) 481

12. S. Katsanevas, P. Morawitz, *Comp. Phys. Comm.* **112** (1998) 227
13. T. Sjöstrand, *Comp. Phys. Comm.* **82** (1994) 74
14. M. Skrzypek, S. Jadach, W. Placzek, Z. Wąs, *Comp. Phys. Comm.* **94** (1996) 216
15. Reports of the working groups on precision calculations for LEP2 Physics, CERN 2000-009
16. H. Anlauf et al., *Comp. Phys. Comm.* **79** (1994) 466
17. S. Jadach, Z. Wąs, *Comp. Phys. Comm.* **36** (1985) 191
18. J.A.M. Vermaseren in "Proceedings of the IVth international Workshop on Gamma Gamma Interactions", Eds. G. Cochard, P. Kessler, Springer Verlag, 1980
19. C. Caso et al., Particle Data Group, *Eur. Phys. J.* **C3** (1998) 1
20. ALEPH Collaboration, "Search for supersymmetry with a dominant R-Parity violating $LL\bar{E}$ coupling in e^+e^- collisions at centre-of-mass energies of 130 GeV to 172 GeV", *Eur. Phys. J.* **C4** (1998) 433
21. S. Dimopoulos, L.J. Hall, *Phys. Lett.* **B 207** (1988) 210; V. Barger, G. F. Giudice, T. Han, *Phys. Rev.* **D40** (1989) 2987; H. Dreiner, S. Lola, published in "Munich/Annecy/Hamburg 1991, Proceedings, e^+e^- collisions at 500 GeV"; separately in "Searches for New Physics", contribution to the LEP2 workshop, 1996, hep-ph/9602207; and "Physics with e^+e^- Linear Colliders", DESY-97-100, hep-ph/9705442
22. ALEPH Collaboration, Study of Fermion pair production in e^+e^- collisions at 130-183 GeV *Euro. Phys. J.* **C12** (2000) 183
23. B.C. Allanach, A. Dedes, H.K. Dreiner, *Phys. Rev.* **D 60** (1999) 075014; G. Bhattacharyya, *Nucl. Phys. Proc. Suppl.* **52A** (1997) 83
24. ALEPH Collaboration, "Search for charginos and neutralinos in e^+e^- collisions at centre-of-mass energies near 183 GeV and constraints on the MSSM parameter space", *Euro. Phys. J.* **C 11** (1999) 193
25. ALEPH Collaboration, "Search for supersymmetry with a dominant R-Parity violating $LQ\bar{D}$ coupling in e^+e^- collisions at centre-of-mass energies of 130 GeV to 172 GeV", *Eur. Phys. J.* **C7** (1999) 383
26. D0 Collaboration, "Search for second generation leptoquark pairs in $p\bar{p}$ collisions at $\sqrt{s} = 1.8$ TeV", *Phys. Rev. Lett.* **84** (2000) 2088; CDF Collaboration, "Search for second generation Leptoquarks in the dimuon plus dijet channel of p collisions at $\sqrt{s} = 1.8$ TeV", *Phys. Rev. Lett.* **81** (1998) 4086; D0 Collaboration, "Search for first generation scalar leptoquark pairs in $p\bar{p}$ collisions at $\sqrt{s} = 1.8$ TeV", *Phys. Rev. Lett.* **80** (1998) 2051; CDF Collaboration, "Search for first generation Leptoquark pair production in $p\bar{p}$ collisions at $\sqrt{s} = 1.8$ TeV", *Phys. Rev. Lett.* **79** (1997) 4327